

Impact of network topology on synchrony of oscillatory power grids

Martin Rohden,¹ Andreas Sorge,¹ Dirk Witthaut,¹ and Marc Timme^{1,2}

¹*Network Dynamics, Max Planck Institute for Dynamics and Self-Organization (MPIDS), 37077 Göttingen, Germany*

²*Faculty of Physics, Georg August University Göttingen, Germany*

(Dated: 27 November 2024)

Replacing conventional power sources by renewable sources in current power grids drastically alters their structure and functionality. The resulting grid will be far more decentralized with an distinctly different topology. Here we analyze the impact of grid topologies on spontaneous synchronization, considering regular, random and small-world topologies and focusing on the influence of decentralization. We employ the *classic model* of power grids modeling consumers and sources as second order oscillators. We first analyze the global dynamics of the simplest non-trivial (two-node) network that exhibit a synchronous (normal operation) state, a limit cycle (power outage) and coexistence of both. Second, we estimate stability thresholds for the collective dynamics of small network motifs, in particular star-like networks and regular grid motifs. For larger networks we numerically investigate decentralization scenarios finding that decentralization itself may support power grids in reaching stable synchrony for lower lines transmission capacities. Decentralization may thus be beneficial for power grids, regardless of their special resulting topology. Regular grids exhibit a specific transition behavior not found for random or small-world grids.

PACS numbers: 05.45.Xt,84.70.+p,89.75.-k

The availability of electric energy fundamentally underlies all aspects of life; thus its reliable distribution is indispensable. The drastic change from our traditional energy system based on fossil fuels to one based dominantly on renewable sources provides an extraordinary challenge for the robust operation of future power grids¹. Renewable sources are intrinsically smaller and more decentralized, thus yielding connection topologies strongly distinct from those of today. How network topologies impact the collective dynamics and in particular the stability of standard grid operation, is still not well understood. In this article, we systematically study how decentralization may influence collective grid dynamics in model oscillatory networks. We first study small network motifs that serve as model system for the larger networks, that are analyzed in this article. We find that, independent of global topological features, decentralized grids are consistently able to reach their stable state for lower transmission line capacities. At least regarding pure topological issues, decentralizing grids may thus be beneficial for operating oscillatory power grids, largely independent of both the original and the resulting grid.

I. INTRODUCTION

The compositions of current power grids undergo radical changes. As of now, power grids are still dominated by big conventional power plants based on fossil fuel or nuclear power exhibiting a large power output. Essentially, their effective topology is locally star-like with transmission lines going from large plants to regional consumers. As more and more renewable power sources contribute, this is about to change and topologies will become more decentralized and more recurrent. The topologies of current grids largely vary, with large differences, e.g. between grids on islands such as Britain and those in continental Europe, or between areas of different population densities. In addition, renewable sources will strongly modify these structures in a yet unknown way. The synchronization dynamics of many power grids with a special topology are well analyzed², such as the British power grid³ or the European power transmission network⁴. The general impact of grid topologies on collective dynamics is not systematically understood, in particular with respect to decentralization.

Here, we study collective dynamics of oscillatory power grid models with a special focus on how a wide range of topologies, regular, small-world and random, influence stability of synchronous (phase-locked) solutions. We analyze the onset of phase-locking between power generators and consumers as well as the local and global stability of the stable state. In particular, we address the question of how phase-locking is affected in different topologies if large power plants are replaced by small decentralized power sources. For our simulations, we model the dynamics of the power grid as a network of coupled second-order oscillators, which are derived from basic equations of synchronous machines⁵. This model bridges the gap between large-scale static network models⁶⁻⁹ on the one hand and detailed component-level models of smaller network¹⁰ on the other. It thus admits systematic access to emergent dynamical phenomena in large power grids.

The article is organized as follows. We present a dynamical model for power grids in Sec. II. The basic dynamic properties, including stable synchronization, power outage and coexistence of these two states, are discussed in Sec. III for elementary networks. These studies reveal the mechanism of self-organized synchronization in a power grid and help understanding the dynamics also for more complex networks. In Sec. IV we present a detailed analysis of large power grids of different topologies. We investigate the onset of phase-locking and analyze the stability of the phase-locked state against perturbations, with an emphasis on how the dynamics depends on the decentralization of the power generators. Stability aspects of decentralizing power networks has been briefly reported before for the British transmission grid³.

II. COUPLED OSCILLATOR MODEL FOR POWER GRIDS

We consider an oscillator model where each element is one of two types of elements, generator or consumer^{5,11}. Every element i is described by the same equation of motion with a parameter P_i giving the generated ($P_i > 0$) or consumed ($P_i < 0$) power. The state of each element is determined by its phase angle $\phi_i(t)$ and velocity $\dot{\phi}_i(t)$. During the regular operation, generators as well as consumers within the grid run with the same frequency $\Omega = 2\pi \times 50\text{Hz}$ or $\Omega = 2\pi \times 60\text{Hz}$. The phase of each element i is then written as

$$\phi_i(t) = \Omega t + \theta_i(t), \tag{1}$$

where θ_i denotes the phase difference to the set value Ωt .

The equation of motion for all θ_i can now be obtained from the energy conservation law, that is the generated or consumed energy P_i^{source} of each single element must equal the energy sum given or taken from the grid plus the accumulated and dissipated energy of this element. The dissipation power of each element is $P_i^{\text{diss}} = \kappa_i(\dot{\phi}_i)^2$, the accumulated power $P_i^{\text{acc}} = \frac{1}{2}I_i\frac{d}{dt}(\dot{\phi}_i)^2$ and the transitional power between two elements is $P_{ij}^{\text{trans}} = -P_{ij}^{\text{max}}\sin(\phi_j - \phi_i)$. Therefore P_i^{source} is the sum of these:

$$P_i^{\text{source}} = P_i^{\text{diss}} + P_i^{\text{acc}} + P_{ij}^{\text{trans}}. \quad (2)$$

An energy flow between two elements is only possible if there is a phase difference between these two. Inserting equation (1) and assuming only slow phase changes compared to the frequency Ω ($|\dot{\theta}_i| \ll \Omega$). The dynamics of the i th machine is given by:

$$I_i\Omega\ddot{\theta}_i = P_i^{\text{source}} - \kappa_i\Omega^2 - 2\kappa_i\Omega\dot{\theta}_i + \sum_j P_{ij}^{\text{max}}\sin(\theta_j - \theta_i). \quad (3)$$

Note that in this equation only the phase differences θ_i to the fixed phase Ωt appear. This shows that only the phase difference between the elements of the grid matters. The elements $K_{ij} = \frac{P_{ij}^{\text{max}}}{I_i\Omega}$ constitute the connection matrix of the entire grid, therefore it decodes whether or not there is a transmission line between two elements (i and j). With $P_i = \frac{P_i^{\text{source}} - \kappa_i\Omega^2}{I_i\Omega}$ and $\alpha_i = \frac{2\kappa_i}{I_i}$ this leads to the following equation of motion:

$$\frac{d^2\theta_i}{dt^2} = P_i - \alpha_i\frac{d\theta_i}{dt} + \sum_j K_{ij}\sin(\theta_j - \theta_i). \quad (4)$$

The equation can now be rescaled with $s = \alpha t$ and new variables $\tilde{P} = P/\alpha^2$ and $\tilde{K} = K/\alpha^2$.

This leads to:

$$\frac{d^2\theta_i}{ds^2} = \tilde{P}_i - \frac{d\theta_i}{ds} + \sum_j \tilde{K}_{ij}\sin(\theta_j - \theta_i). \quad (5)$$

In the stable state both derivatives $\frac{d\theta_i}{dt}$ and $\frac{d^2\theta_i}{dt^2}$ are zero, such that

$$0 = P_i + \sum_j K_{ij}\sin(\theta_j - \theta_i) \quad (6)$$

holds for each element in the stable state. For the sum over all equations, one for each element i , the following holds

$$\sum_i P_i = \sum_{i<j} K_{ij}\sin(\theta_j - \theta_i) + \sum_{i>j} K_{ij}\sin(\theta_j - \theta_i) = 0, \quad (7)$$

because $K_{ij} = K_{ji}$ and the sin-function is antisymmetric. This means it is a necessary condition that the sum of the generated power ($P_i > 0$) equals the sum of the consumed power ($P_i < 0$) in the stable state.

For our simulations we consider large centralized power plants generating $P_i^{\text{source}} = 100$ MW each. A synchronous generator of this size would have a moment of inertia of the order of $I_i = 10^4 \text{ kg m}^2$. The mechanically dissipated power $\kappa_i \Omega^2$ usually is a small fraction of P^{source} only. However, in a realistic power grid there are additional sources of dissipation, especially ohmic losses and because of damper windings¹², which are not taken into account directly in the coupled oscillator model. Therefore we set $\alpha_i = 0.1 \text{ s}^{-1}$ and $P_i = 10 \text{ s}^{-25}$ for large power plants. For a typical consumer we assume $P_i = -1 \text{ s}^{-2}$, corresponding to a small city. For a renewable power plant we assume $P_i = 2.5 \text{ s}^{-2}$. A major overhead power line can have a transmission capacity of up to $P_{ij}^{\text{max}} = 700$ MW. A power line connecting a small city usually has a smaller transmission capacity, such that $K_{ij} \leq 10^2 \text{ s}^{-2}$ is realistic. We take $\Omega = 2\pi \times 50 \text{ Hz}$.

III. DYNAMICS OF ELEMENTARY NETWORKS

A. Dynamics of one generator coupled with one consumer

We first analyze the simplest non trivial grid, a two-element system consisting of one generator and one consumer. This system is analytically solvable and reveals some general aspects also present in more complex systems. This system can only reach equilibrium if equation (7) is satisfied, such that $-P_1 = P_2$ must hold. With $\Delta P = P_2 - P_1$ the equation of motion for this system can be simplified in such a way, that only the phase difference $\Delta\theta = \theta_2 - \theta_1$ and the difference velocity $\Delta\chi := \dot{\Delta\theta}$ between the oscillators is decisive:

$$\begin{aligned}\Delta\dot{\chi} &= \Delta P - \alpha\Delta\chi - 2K \sin \Delta\theta \\ \Delta\dot{\theta} &= \Delta\chi.\end{aligned}\tag{8}$$

Figure 1 shows different scenarios for the two-element system. For $2K \geq \Delta P$ two fixed points come into being 1(a), whose local stability is analyzed in detail below. The system is globally stable as is shown in the bottom area of Fig. 1 (d). For $2K < \Delta P$ the load exceeds the capacity of the link. No stable operation is possible and all trajectories converge to a limit cycle as shown in fig 1 (b) and in the upper area of 1 (d). In the remaining region of

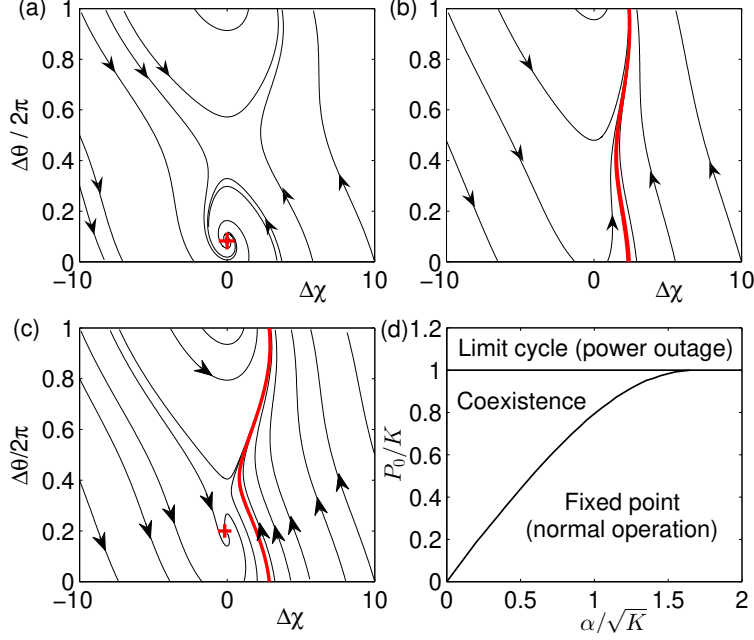


FIG. 1. Dynamics of an elementary network with one generator and one consumer for $\alpha = 0.1s^{-1}$.

- (a) Globally stable phase locking for $P_0 = 1s^{-2}$ and $K = 2s^{-2}$
- (b) Globally unstable phase locking (limit cycle) for $P_0 = 1s^{-2}$ and $K = 0.5s^{-2}$
- (c) Coexistence of phase locking (normal operation) and limit cycle (power outage) for $P_0 = 1s^{-2}$ and $K = 1.1s^{-2}$
- (d) Stability phase diagram in parameter space.

parameter space, the fixed point and the limit cycle coexist such that the dynamics depend crucially on the initial conditions as shown in fig 1 (c) (cf.¹³). Most major power grids are operating close to the edge of stability, i.e. in the region of coexistence, at least during periods of high loads. Therefore the dynamics depends crucially on the initial conditions and static power grid models are insufficient.

Let us now analyze the fixed points of the equations of motion (8) in more detail. In terms of the phase difference $\Delta\theta$, they are given by:

$$\begin{aligned}
 T_1 : \quad & \begin{pmatrix} \Delta\chi^* \\ \Delta\theta^* \end{pmatrix} = \begin{pmatrix} 0 \\ \arcsin \frac{\Delta P}{2K} \end{pmatrix}, \\
 T_2 : \quad & \begin{pmatrix} \Delta\chi^* \\ \Delta\theta^* \end{pmatrix} = \begin{pmatrix} 0 \\ \pi - \arcsin \frac{\Delta P}{2K} \end{pmatrix}.
 \end{aligned} \tag{9}$$

For $\Delta P > 2K$ no fixed point can exist as discussed above. The critical coupling strengths

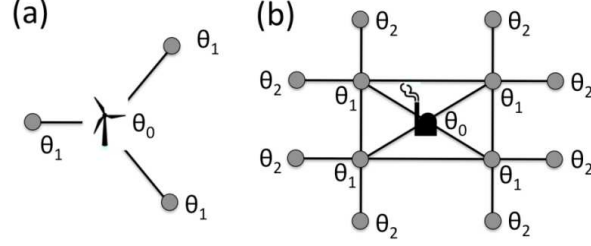


FIG. 2. Motif networks: simplified phase description

K_c is therefore $\Delta P/2$. Otherwise fixed points exist and the system can reach a stationary state. For $\Delta P = 2K$ only one fixed point exists, $T_1 = T_2$, at $(\Delta\chi^*, \Delta\theta^*) = (0, \pi/2)$. It is neutrally stable.

We have two fixed points for $2K > \Delta P$. The local stability of these fixed points is determined by the eigenvalues of the Jacobian of the dynamical system (8), which are given by

$$\lambda_{\pm}^{(1)} = -\frac{\alpha}{2} \pm \sqrt{\left(\frac{\alpha}{2}\right)^2 - \sqrt{4K^2 - \Delta P^2}} \quad (10)$$

at the first fixed point T_1 and

$$\lambda_{\pm}^{(2)} = -\frac{\alpha}{2} \pm \sqrt{\left(\frac{\alpha}{2}\right)^2 + \sqrt{4K^2 - \Delta P^2}} \quad (11)$$

at the second fixed point T_2 , respectively. Depending on K , the eigenvalues at the first fixed point are either both real and negative or complex with negative real values. One eigenvalue at the second fixed point is always real and positive, the other one real and negative. Thus only the first fixed point is stable and enables a stable operation of the power grid. It has real and negative eigenvalues for $K_c < K < K_2 = \sqrt{\frac{\alpha^4}{64} + \frac{\Delta P^2}{4}}$, which is only possible for large α , i.e. the system is overdamped. For $K \geq K_2$ it has complex eigenvalues with a negative real value $|\Re(\lambda)| \equiv \frac{\alpha}{2}$, for which the power grid exhibits damped oscillations around the fixed point. As power grids should work with only minimal losses, which corresponds to $K \geq K_2$, this is the practically relevant setting.

B. Dynamics of motif networks

We discuss the dynamics of the two motif networks shown in Fig. 2. These two can be considered as building blocks of the large-scale quasi-regular network that will be analyzed in

the next section. Fig. 2 (a) shows a simple network, where a small renewable energy source provides the power for $N = 3$ consumer units with $d = 3$ connections. To analyze the most homogeneous setting we assume that all consumers have the same phase θ_1 and a power load of $-P_0$ and all transmission lines have the same capacity K . The power generator has the phase θ_0 and provides a power of NP_0 . The reduced equations of motion then read

$$\begin{aligned}\ddot{\theta}_0 &= N P_0 - \dot{\theta}_0 + dK \sin(\theta_1 - \theta_0), \\ \ddot{\theta}_1 &= -P_0 - \dot{\theta}_1 + K \sin(\theta_0 - \theta_1)\end{aligned}\tag{12}$$

. For this motif class the condition $|N| = |d|$ always holds, such that the steady state is determined by $\sin(\theta_0 - \theta_1) = P_0/K$. The condition for the existence of a steady state is thus $K > K_c = P_0$, i.e. each transmission line must be able to transmit the power load of one consumer unit.

Fig. 2 (b) shows a different network, where $N = 12$ consumer units arranged on a squared lattice with $d_1 = 4$ connections between the central power source (θ_0) and the nearest consumers (θ_1) and $d_2 = 2$ connections between the consumers with phase θ_1 and those with θ_2 . Due to the symmetry of the problem we have to consider only three different phases. The reduced equations of motion then read

$$\begin{aligned}\ddot{\theta}_0 &= N P_0 - \dot{\theta}_0 + d_1 K \sin(\theta_1 - \theta_0), \\ \ddot{\theta}_1 &= -P_0 - \dot{\theta}_1 + d_2 K \sin(\theta_2 - \theta_1) + K \sin(\theta_0 - \theta_1), \\ \ddot{\theta}_2 &= -P_0 - \dot{\theta}_2 + K \sin(\theta_1 - \theta_2).\end{aligned}\tag{13}$$

For the steady state we thus find the relations

$$\begin{aligned}\sin(\theta_0 - \theta_1) &= (NP_0)/(d_1 K) \\ \sin(\theta_1 - \theta_2) &= P_0/K.\end{aligned}\tag{14}$$

The coupling strengths K must now be higher than the critical coupling strengths

$$K_c = \frac{NP_0}{d_1}\tag{15}$$

to enable a stable operation. For the example shown in Fig. 2 (b) we now have a higher critical coupling strength $K_c = 3P_0$ compared to the previous motif for the existence of a steady state. This is immediately clear from physical reasons, as the transmission lines leading away from the power plant now have to serve 3 consumer units instead of just one.

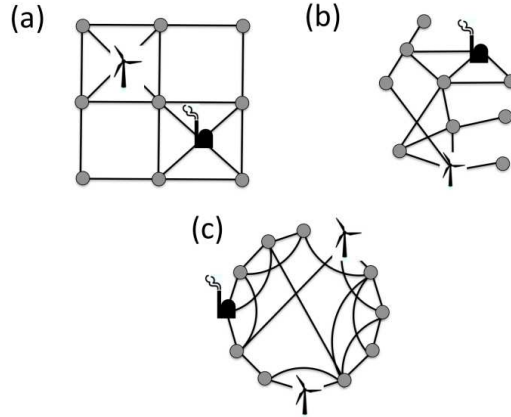


FIG. 3. Small size cartoons of different network topologies: (a) Quasi-regular grid, (b) random network and (c) small-world network.

IV. DYNAMICS OF LARGE POWER GRIDS

A. Network topology

We now turn to the collective behavior of large networks of coupled generators and consumers and analyze how the dynamics and stability of a power grid depend on the network structure. We emphasize how the stability is affected when large power plants are replaced by many small decentralized power sources.

In the following we consider power grids of $N_C = 100$ consumers units with the same power load $-P_0$ each. In all simulations we assume $P_0 = 1s^{-2}$ with $\alpha = 0.1s^{-1}$ as discussed in Sec. II. The demand of the consumers is met by $N_P \in \{0, \dots, 10\}$ large power plants, which provide a power $P_P = 10 P_0$ each. The remaining power is generated by N_R small decentralized power stations, which contribute $P_R = 2.5 P_0$ each. Consumers and generators are connected by transmission lines with a capacity K , assumed to be the same for all connections.

We consider three types of networks topologies, schematically shown in Fig. 3. In a quasi-regular power grid, all consumers are placed on a squared lattice. The generators are placed randomly at the lattice and connected to the adjacent four consumer units (cf. Fig. 3 (a)). In a random network, all elements are linked completely randomly with an average number of six connections per node (cf. Fig. 3 (b)). A small world network is obtained by a standard rewiring algorithm¹⁴ as follows. Starting from ring network, where every element is connected

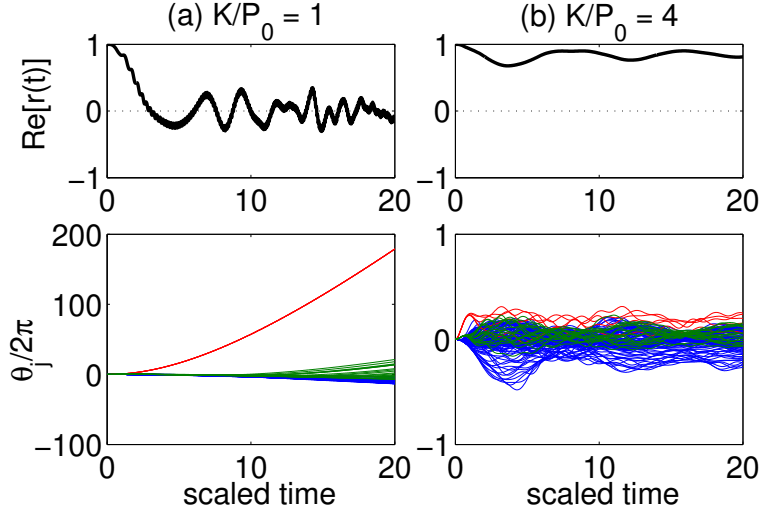


FIG. 4. Synchronization dynamics of a quasi-regular power grid. (a) For a weak coupling the phases $\theta_j(t)$ of the small renewable decentralized generators (green lines) synchronize with the consumers (blue lines), but not the phases of the large power plants (red lines). Thus the order parameter $r(t)$ fluctuates around a zero mean. (b) Global phase-locking of all generators and consumers is achieved for a large coupling strength, such that the order parameters $r(t)$ is almost one.

to its four nearest neighbors, the connections are randomly rewired with a probability of 0.1 (cf. Fig. 3 (c)).

B. The synchronization transition

We analyze the requirements for the onset of phase locking between generators and consumers, in particular the minimal coupling strength K_c . An example for the synchronization transition is shown in Fig. 4, where the dynamics of the phases $\theta_i(t)$ is shown for two different values of the coupling strength K . Without coupling, $K = 0$, all elements of the grid oscillate with their natural frequency. For small values of K , synchronization sets in between the renewable generators and the consumers whose frequency difference is rather small (cf. Fig. 4 (a)). Only if the coupling is further increased (Fig. 4 (b)), all generators synchronize so that a stable operation of the power grid is possible.

The phase coherence of the oscillators is quantified by the order parameter¹⁵

$$r(t) = \frac{1}{N} \sum_j e^{i\theta_j(t)}, \quad (16)$$

which is also plotted in Fig. 4. For a synchronous operation, the real part of the order parameters is almost one, while it fluctuates around zero otherwise. In the long time limit, the system will either relax to a steady synchronous state or to a limit cycle where the generators and consumers are decoupled and $r(t)$ oscillates around zero. In order to quantify synchronization in the long time limit we thus define the averaged order parameter

$$r_\infty := \lim_{t_1 \rightarrow \infty} \lim_{t_2 \rightarrow \infty} \frac{1}{t_2} \int_{t_1}^{t_1+t_2} r(t) dt. \quad (17)$$

In numerical simulations the integration time t_2 must be finite, but large compared to the oscillation period if the system converges to a limit cycle. Furthermore we consider the averaged squared phase velocity

$$v^2(t) = \frac{1}{N} \sum_j \dot{\theta}_j(t)^2, \quad (18)$$

and its limiting value

$$v_\infty^2 := \lim_{t_1 \rightarrow \infty} \lim_{t_2 \rightarrow \infty} \frac{1}{t_2} \int_{t_1}^{t_1+t_2} v^2(t) dt \quad (19)$$

as a measure of whether the grid relaxes to a stationary state. These two quantities are plotted in Fig. 5 as a function of the coupling strength K/P_0 for 20 realizations of a quasi-regular network with 100 consumers and 40 % renewable energy sources. The onset of synchronization is clearly visible: If the coupling is smaller than a critical value K_c no steady synchronized state exists and $r_\infty = 0$ by definition. Increasing K above K_c leads to the onset of phase locking such that r_∞ jumps to a non-zero value. The critical value of the coupling strength is found to lie in the range $K_c/P_0 \approx 3.1 - 4.2$, depending on the random realization of the network topology.

The synchronization transition is quantitatively analyzed in Fig. 6. We plotted r_∞ and v_∞ for three different network topologies averaged over 100 random realizations for each amount of decentralized energy sources for every topology. The synchronization transition strongly depends on the structure of the network, and in particular the amount of power provided by small decentralized energy sources. Each line in Fig. 4 corresponds to a different fraction of decentralized energy $1 - N_P/10$, where N_P is the number of large conventional power plants feeding the grid. Most interestingly, the introduction of small decentralized power sources (i.e. the reduction of N_P) promotes the onset of synchronization. This phenomenon is most obvious for the random and the small-worlds structures.

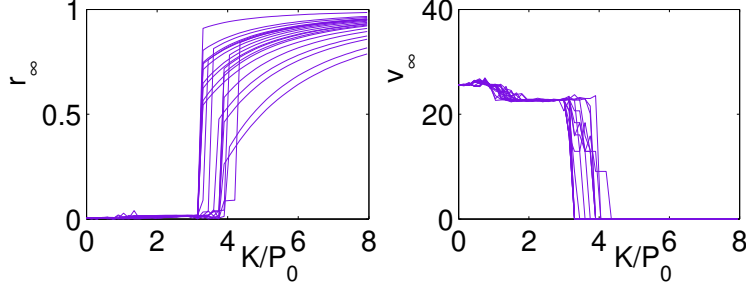


FIG. 5. The synchronization transition as a function of the coupling strength K : The order parameter r_∞ (left-hand side) and the phase velocity v_∞ (right-hand side) in the long time limit. The dynamics has been simulated for 20 different realizations of a quasi-regular network consisting of 100 consumers, $N_P = 6$ large power plants and $N_R = 16$ small power generators.

Let us first analyze the quasi-regular grid in the limiting cases $N_P = 10$ (only large power plants) and $N_P = 0$ (only small decentralized power stations) in detail. The existence of a synchronized steady state requires that the transmission lines leading away from a generator have enough capacity to transfer the complete power, i.e. $10 P_0$ for a large power plant and $2.5 P_0$ for a small power station. In a quasi-regular grid every generator is connected with exactly four transmission lines, which leads to the following estimate for the critical coupling strength (cf. equation 15):

$$\begin{aligned}
 K_c &= 10P_0/4 & \text{for } N_P = 10, \\
 K_c &= 2.5P_0/4 & \text{for } N_P = 0.
 \end{aligned}
 \tag{20}$$

These values only hold for a completely homogeneous distribution of the power load and thus rather present a lower bound for K_c in a realistic network. Indeed, the numerical results shown in Fig. 6 (a) yield a critical coupling strength of $K_c \approx 3.2 \times P_0$ and $K_c \approx 1 \times P_0$, respectively.

For networks with a mixed structure of power generators ($N_P \in \{1, \dots, 9\}$) we observe that the synchronization transition is determined by the large power plants, i.e. the critical coupling is always given by $K_c \approx 3.2 \times P_0$ as long as $N_P \neq 0$. However, the transition is now extremely sharp – the order parameter does not increase smoothly but rather jumps to a high value. This results from the fact that all small power stations are already strongly synchronized with the consumers for smaller values of K and only the few large power plants are missing. When they finally fall in as the coupling strength exceeds K_c , the order

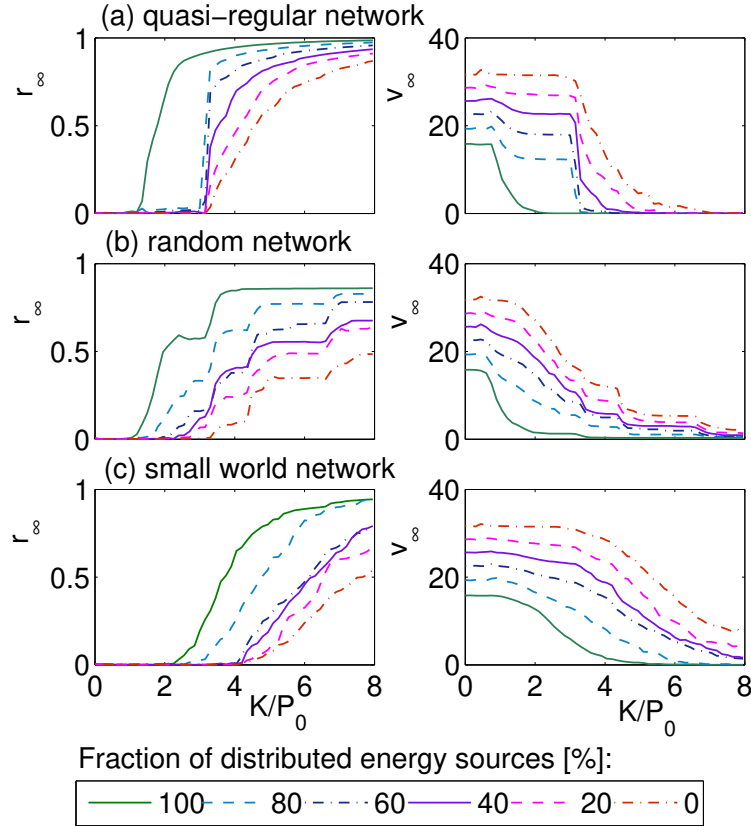


FIG. 6. The synchronization transition for different fractions of decentralized energy sources $1 - N_P/10$ feeding the grid and for different network topologies: (a) Quasi-regular grid, (b) random network and (c) small-world network. The order parameter r_∞ and the phase velocity v_∞ (cf. Fig. 5) have been averaged over 100 realizations for each network structure and each fraction of decentralized sources.

parameter r immediately jumps to a large value.

The sharp transition at K_c is a characteristic of the quasi-regular grid. For a random and a small-world network different classes of power generators exist, which are connected with different numbers of transmission lines. These different classes get synchronized to the consumers one after another as K is increased, starting with the class with the highest amount of transmission lines to the one with fewest. Therefore we observe a smooth increase of the order parameter r .

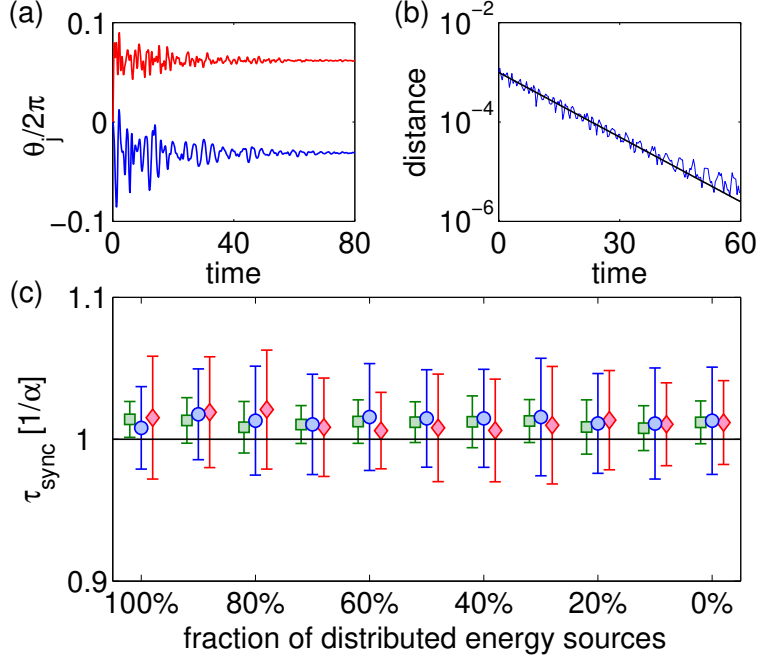


FIG. 7. Relaxation to the synchronized steady state: (a) Illustration of the relaxation process ($K/P_0 = 10$ and $N_P = 10$). We have plotted the dynamics of the phases θ_j only for one generator (red) and one consumer (blue) for the sake of clarity. (b) Exponential decrease of the distance to the steady state (blue line) and a fit according to $d(t) \sim e^{-t/\tau_{\text{sync}}}$ (black line). (c) The synchronisation time τ_{sync} as a function of the fraction of decentralized energy sources $1 - N_P/10$ for a regular (\circ), a random (\square) and a small-world grid (\diamond). Cases where the system does not relax have been discarded.

C. Local stability and synchronization time

A sufficiently large coupling of the nodes leads to synchronization of all nodes of a power grid as shown in the preceding section. Starting from an arbitrary state in the basin of attraction, the network relaxes to the stable synchronized state with a time scale τ_{sync} . For instance, Fig. 7 (a) shows the damped oscillations of the phase $\theta_j(t)$ of a power plant and a consumer in a quasi-regular grid with $K = 10$ and $N_P = 10$. In order to quantify the relaxation, we calculate the distance to the steady state

$$d(t) = \left(\sum_{i=1}^N d_1^2(\theta_i(t), \theta_{i,\text{st}}) + d_2^2(\dot{\theta}_i(t), \dot{\theta}_{i,\text{st}}) \right)^{\frac{1}{2}}, \quad (21)$$

where the subscript 'st' denotes the steady state values. For the phase velocities d_2 denotes the common Euclidian distance $d_2^2(\dot{\alpha}, \dot{\beta}) = |\dot{\alpha} - \dot{\beta}|^2$, while the circular distance of the phases is defined as

$$d_1(\alpha, \beta) = 1 - \cos(\alpha - \beta). \quad (22)$$

The distance $d(t)$ decreases exponentially during the relaxation to the steady state as shown in Fig. 7 (b). The black line in the figure shows a fit with the function $d(t) = d_0 \exp(-t/\tau_{\text{sync}})$. Thus synchronization time τ_{sync} measures the local stability of the stable fixed point, being the inverse of the stability exponent λ (cf. the discussion in Sec. III A).

Fig. 7 (c) shows how the synchronization time depends on the structure of the network and the mixture of power generators. For several paradigmatic systems of oscillators, it was recently shown that the time scale of the relaxation process depends crucially on the network structure¹⁶. Here, however, we have a network of *damped* second order oscillators. Therefore the relaxation is almost exclusively given by the inverse damping constant α^{-1} . Indeed we find $\tau_{\text{sync}} \gtrsim \alpha^{-1}$. For an elementary grid with two nodes only, this was shown rigorously in Sec. III A. As soon as the coupling strength exceeds a critical value $K > K_2$, the real part of the stability exponent is given by α , independent of the other system parameters. A different value is found only for intermediate values of the coupling strength $K_c < K < K_2$. Generally, this remains true also for a complex network of many consumers and generators as shown in Fig. 7 (c). For the given parameter values we observe neither a systematic dependence of the synchronization time τ_{sync} on the network topology nor on the number of large (N_P) and small (N_R) power generators. The mean value of τ_{sync} is always slightly larger than the relaxation constant α^{-1} . Furthermore, also the standard deviation of τ_{sync} for different realizations of the random networks is only maximum 3 percent of the mean value. A significant influence of the network structure on the synchronization time has been found only in the weak damping limit, i.e. for very large values of P_0/α and K/α .

D. Stability against perturbations

Finally, we test the stability of different network structures against perturbations on the consumers side. We perturb the system after it has reached a stable state and measure if the system relaxes to a steady state after the perturbation has been switched off again. The perturbation is realized by an increased power demand of each consumer during a short

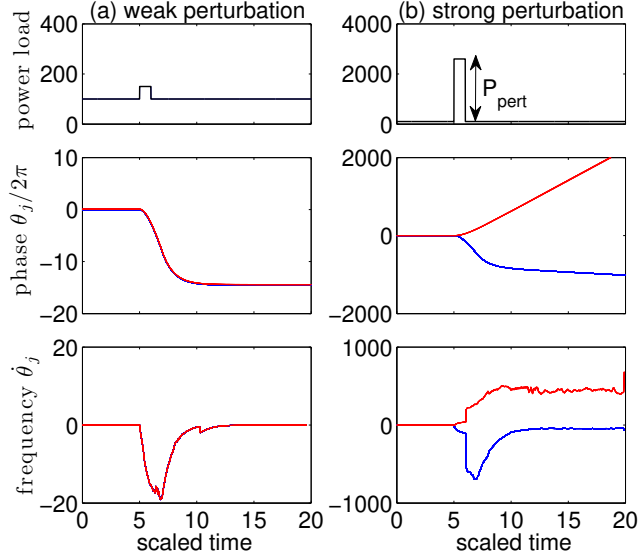


FIG. 8. Weak and strong perturbation. The upper panels show the time-dependent power load of the consumers. A perturbation of strength P_{pert} is applied in the time interval $t \in [5, 6]$. The lower panels show the resulting dynamics of the phase θ_j and the frequency $\dot{\theta}_j$ of the consumers (blue lines) and the power plants (red lines). The dynamics relaxes back to a steady state after the perturbation for a weak perturbation (a), but not for a strong perturbation (b). In both cases we assume a regular grid with $N_P = 10$.

time interval ($\Delta t = 10s$) as illustrated in the upper panels of Fig. 8. Therefore the condition of 7 is violated and the system cannot remain in its stable state. After the perturbation is switched off again, the system relaxes back to a steady state or not, depending on the strength of the perturbation. Fig. 8 shows examples of the dynamics for a weak (a) and strong (b) perturbation, respectively.

These simulations are repeated 100 times for every value of the perturbation strength for each of the three network topologies. We then count the fraction of networks which are unstable, i.e do not relax back to a steady state. The results are summarized in Fig. 9 for different network topologies. The figure shows the fraction of unstable grids as a function of the perturbation strength and the number of large power plants. For all topologies, the best situation is found when the power is generated by both large power plants and small power generators. An explanation is that the moment of inertia of a power source is larger if it delivers more power, which makes it more stable against perturbations. On the other hand, a more distributed arrangement of power stations favors a stable synchronous operation as

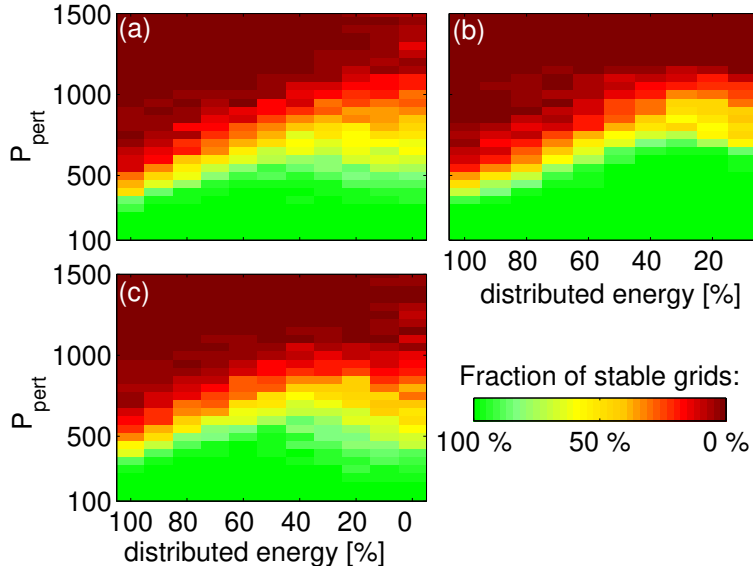


FIG. 9. Robustness of a power grid. The panels show the fraction of random grids which are unstable against a perturbation as a function of the perturbation strength P_{pert} and the fraction of decentralized energy $1 - N_P/10$. (a) Quasi-regular grid, (b) random network and (c) small-world network.

shown in Sec. III B.

Furthermore, the variability of the power grids is stronger for low values of N_P , i.e. few large power plants. The results do not change much for networks which many power sources (i.e. high N_P) because more power sources are distributed in the grid. Thus the random networks differ only weakly and one observes a sharp transition between stable and unstable. This is different if only few large power plant are present in the network. For certain arrangements of power stations the system can reach a steady state even for strong perturbations. But the system can also fail to do so with only small perturbations if the power stations are clustered. This emphasizes the necessity for a careful planning of the structure of a power grid to guarantee maximum stability.

V. CONCLUSION AND OUTLOOK

In the present article we have analyzed a dynamical network model for the dynamics of a power grid. Each element of the network is modeled as a second-order oscillator similar to a synchronous generator or motor. Such a model bridges the gap between a microscopic

description of electric machines and static models of large supply networks. It incorporates the basic dynamical effects of coupled electric machines, but it is still simple enough to simulate and understand the collective phenomena in complex network topologies.

The basic dynamical mechanisms were explored for elementary network structures. We showed that a self-organized phase-locking of all generators and motors in the network is possible. However, this requires a strong enough coupling between elements. If the coupling is decreased, the synchronized steady state of the system vanishes.

We devoted the second part to a numerical investigation of the dynamics of large networks of coupled generators and consumers, with an emphasis on self-organized phase-locking and the stability of the synchronized state for different topologies. It was shown that the critical coupling strength for the onset of synchronization depends strongly on the degree of decentralization. Many small generators can synchronize with a lower coupling strength than few large power plants for all considered topologies. The relaxation time to the steady state, however, depends only weakly on the network structure and is generally determined by the dissipation rate of the generators and motors. Furthermore we investigated the robustness of the synchronized steady state against a short perturbation of the power consumption. We found that networks powered by a mixture of small generators and large power plants are most robust. However, synchrony was lost only for perturbations at least five times their normal energy consumption in all topologies for the given parameter values.

For the future it would be desirable to gain more insight into the stability of power grids regarding transmission line failures, which is not fully understood yet¹⁷. For instance, an enormous challenge for the construction of future power grids is that wind energy sources are planned predominantly at seashores such that energy is often generated far away from most consumers. That means that a lot of new transmission lines will be added into the grid and such many more potential transmission line failures can occur. Although the general topology of these future power grids seem to be not that decisive for their functionality, the impact of including or deleting single links is still not fully understood and unexpected behaviors can occur¹⁸. Furthermore it is highly desirable to gain more insight into collective phenomena such as cascading failures to prevent major outages in the future.

REFERENCES

- ¹D. Butler, *Nature* **445**, 586 (2007).
- ²A. E. Motter, S Myers, M. Anghel and T. Nishikawa, *Nature Phys.* **9**, 191-197 (2013).
- ³M. Rohden, A.Sorge. M. Timme, D. Witthaut, *Phys. Rev. Lett.* **109**, 064101 (2012).
- ⁴S. Lozano, L. Buzna, A. Diaz-Guilera, *Eur. Phys. J. B* **85**, 231 (2012).
- ⁵G. Filatrella, A. H. Nielsen, and N. F. Pedersen, *Eur. Phys. J. B* **61**, 485 (2008).
- ⁶A. E. Motter and Y.-C. Lai, *Phys. Rev. E* **66**, 065102 (2002).
- ⁷M. Schäfer, J. Scholz, and M. Greiner, *Phys. Rev. Lett.* **96**, 108701 (2006).
- ⁸I. Simonsen, L. Buzna, K. Peters, S. Bornholdt, and D. Helbing, *Phys. Rev. Lett.* **100**, 218701 (2008).
- ⁹D. Heide, M. Schäfer, and M. Greiner, *Phys. Rev. E* **77**, 056103 (2008).
- ¹⁰See, e.g., the power system simulation packages PSS/E (<http://www.energy.siemens.com>) or EUROSTAG (<http://www.eurostag.be>).
- ¹¹P. Kundur, *Power system stability and control*, McGraw-Hill, New York (1994).
- ¹²J. Machowski, J. Bialek and J. Bumby, *Power System Dynamics: Stability and Control*, pages: 172 ff, Wiley, (2009).
- ¹³H. Risken, *The Fokker-Planck Equation*, Springer, Berlin Heidelberg (1996).
- ¹⁴D. J. Watts and S. H. Strogatz, *Collective dynamics of 'small-world' networks*, *Nature* **393**, 440 (1998).
- ¹⁵S. H. Strogatz, *Physica D* **143**, 1 (2000).
- ¹⁶C. Grabow, S. Hill, S. Grosskinsky, and M. Timme, *Europhys. Lett.* **90**, 48002 (2010).
- ¹⁷P. Menck, J. Heitzig, N. Marwan and J. Kurths, *Nature Phys.* **9**, 89-92 (2013).
- ¹⁸D. Witthaut and M. Timme, *New J. Phys.* **14**, 083036 (2012).